研究論文

Effect of Low Temperature and Single Overload on Fatigue Crack Growth Behavior of Cr-Mo Steel Weldments

Jae Kyoo Lim* and Yon Jig Kim**

Cr-Mo강 용접부의 피로균열 성장거동에 미치는 저온도와 단일과대하중의 영향

임 재 규*·김 연 직**

Keywords ; Single Overload(단일과대하중), Low Climatic Temperature(저온:-45℃), Fatigue Crack Growth Behavior(피로균열성장거동), Stress Ratio(응력비), Welding HAZ(용접열영향부), Retardation Cycle(지연싸이클), Constant Amplitude Fatigue(일정진폭피로)

-초 록-

일정진폭하중과 과대하중비 2.5의 단일 인장과대하중에 의한 4140강 용접부의 피로균열성장거동을 실온과 -45℃의 저온에서 피로시험과 파면관찰을 통하여 고찰하였다. 이때, 용접부 미시조직의 영향을 평가하기 위해 모재(parent metal), 열영향부(as-welded HAZ), 열처리된 열영향부(PWHT HAZ)로 나누어 응력비 0과 0.5로 CT시험편을 이용하여 피로시험을 실시하였다.

피로균열성장거동은 재료의 미시조직과 온도변화보다는 응력비에 크게 영향을 받았으며, 단일 과대하중에 의한 피로균열성장 지연효과가 모든 재료에서 상당히 크게 나타났다. 전자현미경에 의한 피로파면 관찰결과, 실온에서는 연성의 스트라이에이숀과 -45℃에서는 의벽개파면과 같은 피로균열성장거동을 나타내고 있다.

Abstract

Fatigue crack growth behavior under a constant amplitude loading and single tensile overloads with an OLR of 2.5 was studied for 4140 steel submerged arc weldment at both room

* 정회원, 전북대학교 기계공학부
** 비회원, 전북대학교 기계공학부

temperature and -45℃. Compact tension type, CT, specimens were used with the load ratio, R, of approximately zero and 0.5. Three material conditions were evaluated namely: parent metal, as-welded HAZ and PWHT HAZ. The load ratio, R, had the greatest influence on the fatigue crack growth behavior, while material condition and temperature had little influence. All material conditions responded favorably to the single tensile overloads with fatigue crack growth retardation. SEM examination revealed ductile quasi-striation fatigue crack growth morphology at room temperature and quasi-cleavage at -45℃.

1 INTRODUCTION

A weldment, especially the Heat Affected Zone (HAZ), is a very complicated and variable structure formed from different thermal and environmental conditions [1,2]. These complexities involve inherent mechanical behavior such as strength, ductility, hardness and fracture toughness. In addition, three dimensional residual stress/strain can result in significant decrease of fracture toughness in the HAZ [3~6].

Most welded structures and components are subjected to variable amplitude loading. Defects in weldments serve as sites for the initiation of fatigue cracks that propagate under cyclic loading to the point that unstable fracture can occur. High tensile overloads followed by low amplitude loading can involve appreciable retardation of fatigue crack growth. This retardation has been attributed to crack tip and crack closure [7]. In order to better calculate fatigue crack growth life in weldments, this retardation influence must be known quantitatively.

In addition, welded structures and components in cold areas may be subjected to low climatic temperatures of -45℃ or below. For safe use of such structures and components at low temperature it is necessary to prevent unstable fractures induced by fatigue cracks growing from weld defects [8,9]. This research thus focuses on fatigue crack growth behavior of 4140 steel weldments at room temperature and at a typical low climatic temperature of -45℃. This includes the parent metal, the as-welded HAZ and the HAZ subjected to PWHT. Constant amplitude and single overloads fatigue crack growth behavior in Region II was evaluated for the above three material conditions at room temperature and -45℃ for load ratios, R = Pmin/Pmax, of approximately zero and 0.5. Thus twelve different test conditions were evaluated.

2 TEST MATERIALS AND PROCEDURES

The parent material used in this research was 4140 vacuum degassed steel. Chemical composition and monotonic tensile properties in the rolled direction are given in Table 1 and 2 respectively. A 4140 steel plate with 25mm thickness was cut to 150 × 610mm sections and a U-shaped groove, 610mm long, was cut

Tible 1 Chemical Composition, % weight

	C	Mn	P	S	Si	Ni	Cr	Mo	Ti	V	Cu
4140 steel	0.39	0.81	0.005	0.016	0.11	0.11	0.90	0.17	---	0.04	---
Electrode	0.67	1.57	0.008	0.006	0.38	1.65	0.02	0.35	<0.01	<0.01	0.096
Deposit	0.07	1.38	0.013	0.006	0.31	1.42	0.09	0.30	<0.01	<0.01	0.11

Tible 2 Monotonic Tensile Properties

Property	4140 steel	weld deposit
Ultimate Strength, Su-Mpa	577	772
0.2% Yield Strength, Sy-MPa	388	598
True Fracture Stress, σ_f-MPa	1049	1177
True Fracture Strain, ε_f	0.33	0.24
Reduction in Area-%	54	42

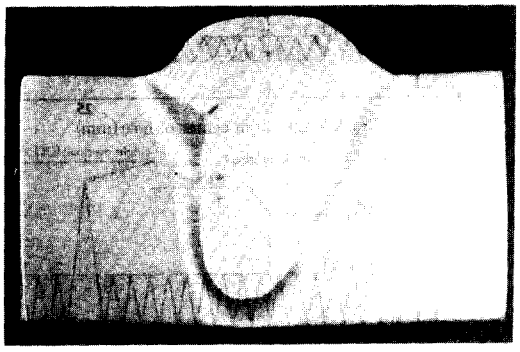

Fig. 1 A typical macroetched cross section of weldment

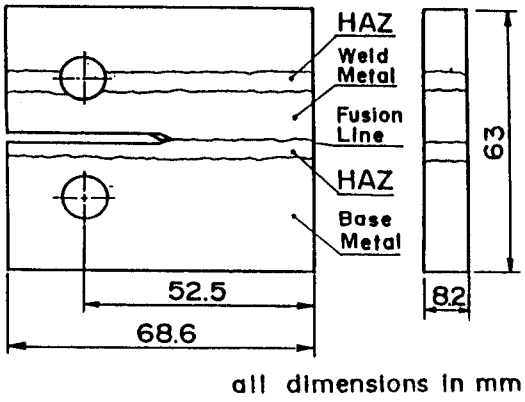

Fig. 2 Compact tension type, CT, specimen

perpendicular to the rolled direction. The U groove was then welded using an automatic submerged arc welder with two passes. A typical macroetched cross section of weldment is shown in Fig. 1. Chevron notched CT specimens were machined from the welded plate as shown in Fig. 2. They were machined so that fatigue cracks would grow through HAZ parallel to the weld direction and perpendicular to the rolled direction. Heat treatment was performed on the welded material CT specimens as follows : heating rate = 220℃/hr, heating temperature = 650℃, hold time = 1hr and cooling rate = 110℃/hr.

The microstructures of the 4140 parent metal and the weld HAZ, are shown in Fig. 3. The microstructures of the 4140 parent metal consists of typical martensite structure with finely dispersed alloy carbides. The HAZ near the fusion line has a coarse-grained microstructure.

Fatigue crack growth tests were performed at room temperature and -45℃ using an 89 kN

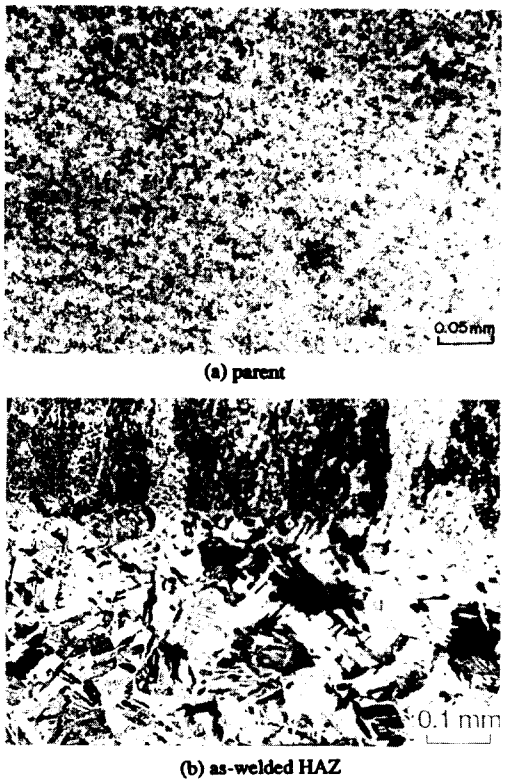

Fig. 3 Microstructures of weld HAZ material (a) parent metal (b) as-welded HAZ

Table 3 Welding Conditions for Submerged Arc Welding

Heat Input	30KJ/cm
Preheating Temperature	200℃
Current	500A
Voltage	30V
Welding Speed	30cm/min
Wire Diameter	2.4mm

closed-loop electrohydraulic test system under load control. Prior to specimen mounting , the tip of the chevron notch was sharpened using a razor blade for quicker crack initiation. One side of each specimen was polished in the crack growth region with progressively finer emery paper to 600 grit. Low temperature tests were performed in an automated CO_2 chamber. Cracks were monitored on polished surfaces using a 33X traveling microscope with stroboscopic illumination. Constant amplitude test was carried out load ratios, R = Pmin/Pmax, of approximately zero and 0.5 using a positive haversine wave with frequencies between 15 and 25 Hz. The fatigue crack growth rate under a constant amplitude ranged from 10^{-8} to 10^{-6} m/cycle and hence was in region Ⅱ, i.e., the Paris log-log linear region. Single tensile overloads were applied at a crack length of 25mm with an overload ratio(OLR) of 2.5 as shown in Fig. 4. Overloads were applied with a ramp wave at 0.125 Hz. All tests were terminated when the crack growth rate became too great to accurately measure the crack length or when the uncracked ligament of the specimen(w-a) ceased to be predominately elastic. All fatigue specimens were precracked approximately 2mm to a total crack length, a, of 22mm. Precracking was usually done in three load shedding steps as shown in Fig. 4. The reduction of Pmax between load steps was less than 20% according to ASTM standard E647. The maximum stress intensity factor, Kmax, just prior to overload was 23.5MPa$(m)^{1/2}$ and the overload stress intensity factor, K_{OL}, was 59 MPa

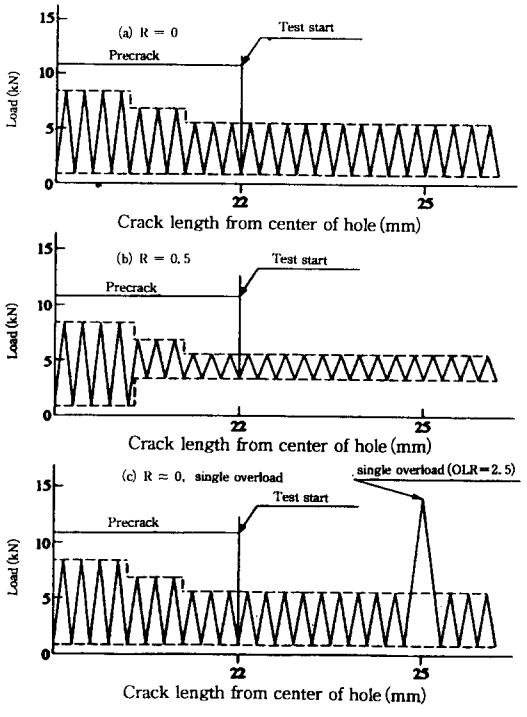

Fig. 4 Load spectrum for precracking, constant load amplitude and tensile overload

$(m)^{1/2}$. Crack length a, versus applied cycle N, data were reduced to da/dN versus △K using a second order incremental polynomial method for a constant load amplitude tests and a secant method for single overload tests.

3 TEST RESULTS AND DISCUSSION

3.1 The effect of low temperature

Fig. 5 shows the temperature and stress ratio effect on the fatigue crack growth behavior for the parent metal, crack length a, versus applied cycles, N. The constant amplitude fatigue crack growth curves are smooth and continuous and fatigue crack grows slowly at R ≈ 0 and low temperature rather than R = 0.5 and room

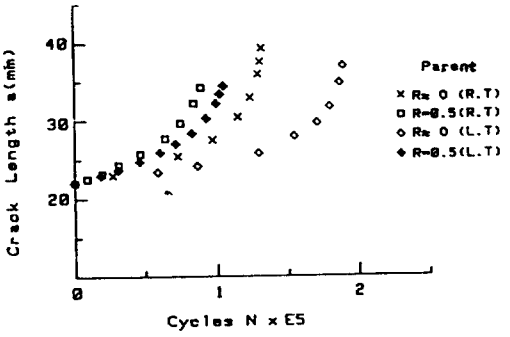

Fig. 5 Fatigue crack growth for parent metal

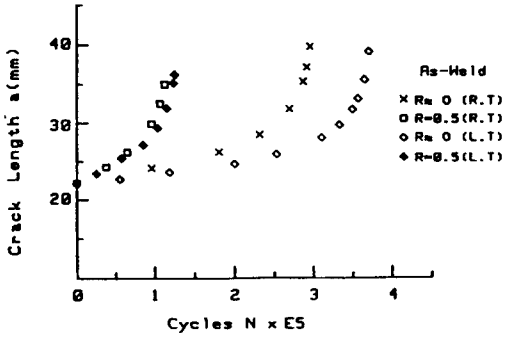

Fig. 6 Fatigue crack growth for as-weld HAZ

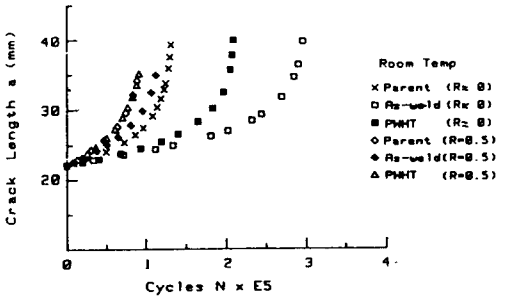

Fig. 7 Fatigue crack growth for room temperature

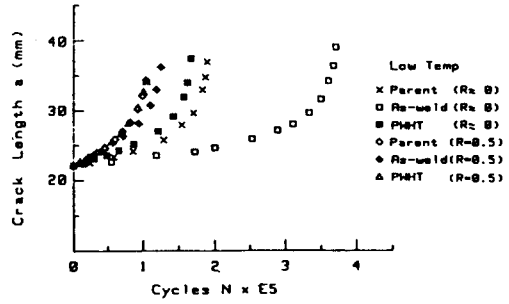

Fig. 8 Fatigue crack growth for low climatic temperature

temperature.

Fig. 6 shows the fatigue crack growth curves of the welded HAZ. Fatigue crack at the HAZ grows slowly at R $\approx$ 0 and low temperature rather than R = 0.5 and room temperature. And then, the effect of stress ratio on the fatigue crack growth at as-welded HAZ is higher than that at parent metal and the effect of the temperature on the fatigue crack growth at as-welded HAZ does not appear nearly at stress ratio of R = 0.5. From Fig. 7 and 8, the effect of the three material conditions on the constant amplitude fatigue crack growth is shown by crack length a, versus applied cycles, N. Fig. 7 shows the curves at room temperature. Fatigue crack grows slowly according to the order of parent metal, PWHT HAZ and as-welded HAZ material. Fig. 8 shows the curves at the low temperature of -45℃. Fatigue crack growth at the parent and PWHT HAZ is nearly same but that of the as-welded HAZ material at the stress ratio of R $\approx$ 0 is the slowest because the strength of welding HAZ. The constant amplitude crack length a, versus applied cycles N, curves are smooth and continuous for all twelve test conditions.

Fig. 9 and 10 show the fatigue crack growth rate as a function of $\triangle$K. Fatigue crack growth rate, da/dN versus $\triangle$K curves for the three material conditions, two temperatures and two R ratios are shown in Fig. 9. The figure is separated for the three different material conditions. For a given material condition, da/dN varies by less than a factor of four for the two R ratios and two temperatures. Most data , however, are within the scatter band closer to two or less. For better interpretation of Fig. 9, all room temperature data have open data points and -45℃ data have closed data points. It is evident then, for a given material

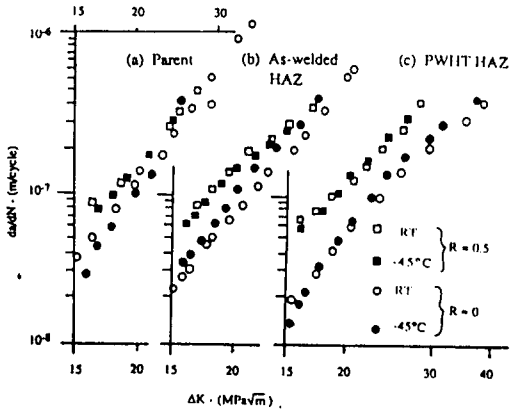

Fig. 9 Fatigue crack growth rate versus ΔK for each material

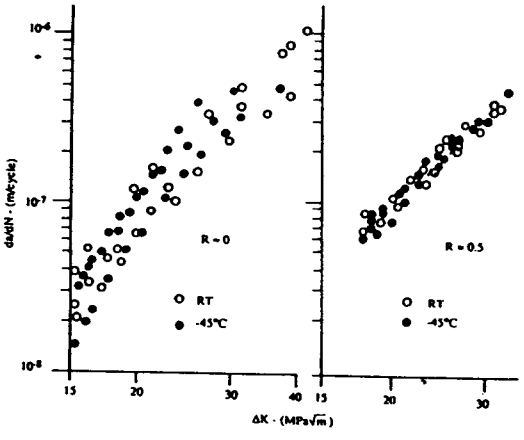

Fig. 10 Fatigue crack growth rate versus ΔK for each R ratio for all material conditions

condition and R ratio, that temperature effect has little or no influence on the fatigue crack growth behavior at Rigion Ⅱ. However, the R ratio did influence on the fatigue crack growth behavior. For a given ΔK, R = 0.5 has always greater fatigue crack growth rates than for R ≈ 0. Fig. 10 shows the superposition of all the fatigue crack growth behavior for a given R ratio. For R ≈ 0, the scatter band for the three material conditions and two temperatures is less than 2.5 to 1 and for R = 0.5 the scatter band is less than 1.5 to 1. This clearly shows that these three material conditions and two temperatures have very similar fatigue crack growth resistance in rigion Ⅱ. The principal factor for a constant amplitude tests appears to be the R ratio and not the material behavior.

3.2 The effect of single overload on fatigue crack growth

The constant amplitude and effect of single tensile overload on the crack growth under a constant load amplitude is shown in Fig. 11 for all R ≈ 0 tests and Fig. 12 for all R = 0.5 respectively. Since each test started at a = 22mm with the same Pmax for both R ratios, and each single tensile overload test had the same overload applied at a = 25mm, followed by the same Pmax value, these two figures provide substantial comparative results without reverting to da/dN versus ΔK curves. In Fig. 11 and 12, the constant amplitude data are represented by open data points and labeled no overload, and the overload data are represented by solid data points or crosses within the symbol. Also for a given material condition, data points with the same shape are used for the constant amplitude test and for the overload test. The general schematic 'a' versus 'N' curves for the no overload curves and the overload curve can be seperated by the number of retardation cycles, NR, where NR is the horizontal displacement of the 'a' versus 'N' curve following a single tensile overload. From Fig. 11 and 12 the overload cycles to failure for a given R ratio fell within a factor of about 2.5 or less for all material test conditions. This again is a rather small variation between materials. The number of cycles of retardation, NR, versus R ratio varies from about 2×10^5 to 6×10^5 cycles. This represents fatigue crack growth life increases from about 400 to 600% for R ≈ 0 and 150 to 300% for R = 0.5. This also indicates that all the material conditions investigated respond favorably to the single tensile overloads. In general, the R = 0.5 tests have a greater number of retardation cycles than for R ≈ 0, however increased the

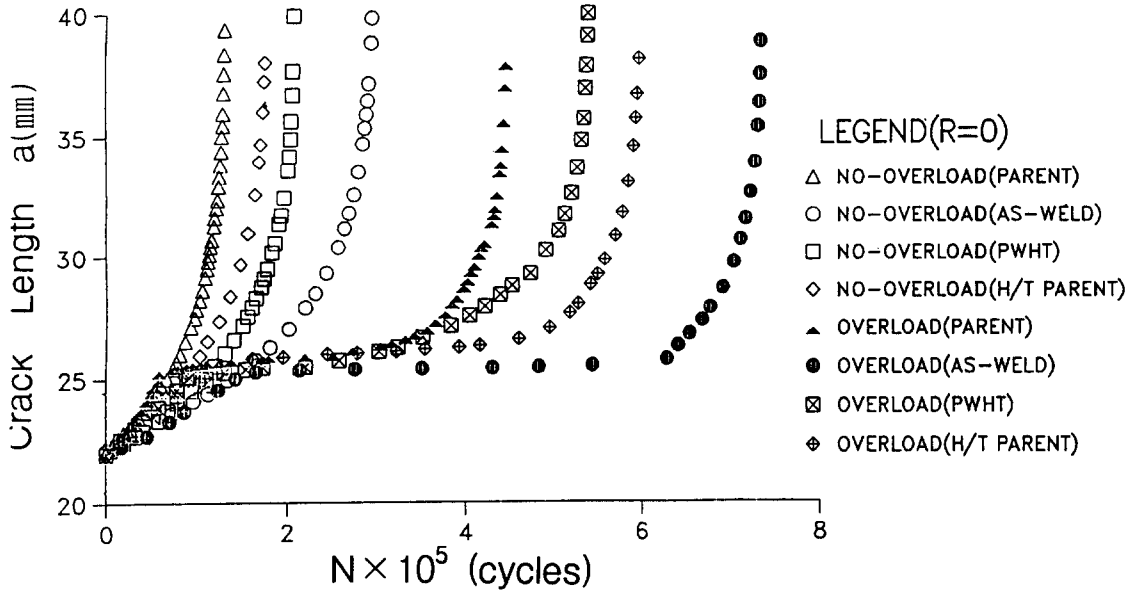

Fig. 11 Crack growth for no overload and single overload conditions, R ≈ 0

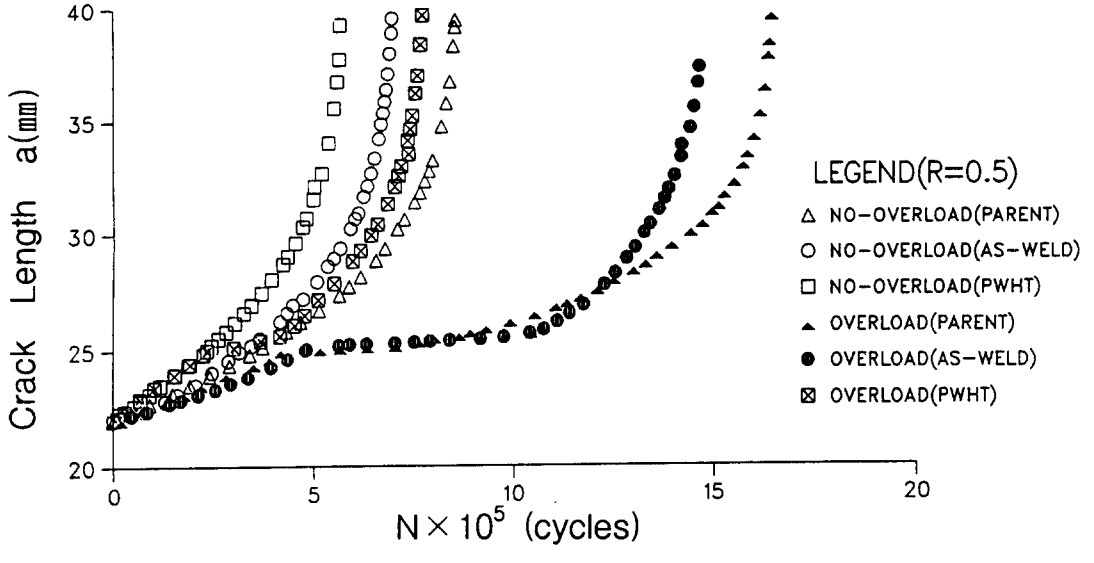

Fig. 12 Crack growth for no overload and single overload conditions, R = 0.5

percent in fatigue life is better for R ≈ 0 tests. The as-welded HAZ material with its higher strength has the greatest response to the single overloads compared to the other lower strength material as shown in Figs. 11 and 12. However, the differences in fatigue crack growth for the as-welded HAZ versus the other material must also incorporate residual stresses that have not been relaxed. In fact, as-welded HAZ material and PWHT HAZ material have the same microstructure, but differ essentially in the residual stresses. Thus both the strength, R ratio and residual stresses are involved with the fatigue crack growth retardation.

The 'a' versus 'N' data for all tests are reduced to da/dN versus △K. Typical results for the no overload and overload conditions are shown in Fig. 13 for the parent metal. Crack growth rates prior to the single tensile overload are above 10^{-8} m/

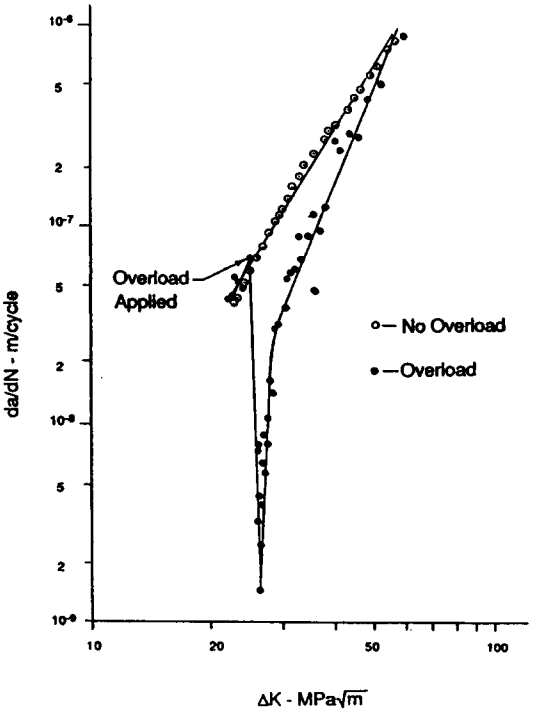

Fig. 13 Fatigue crack growth rate versus Δ K for no overload and single overload, parent metal, R ≈ 0

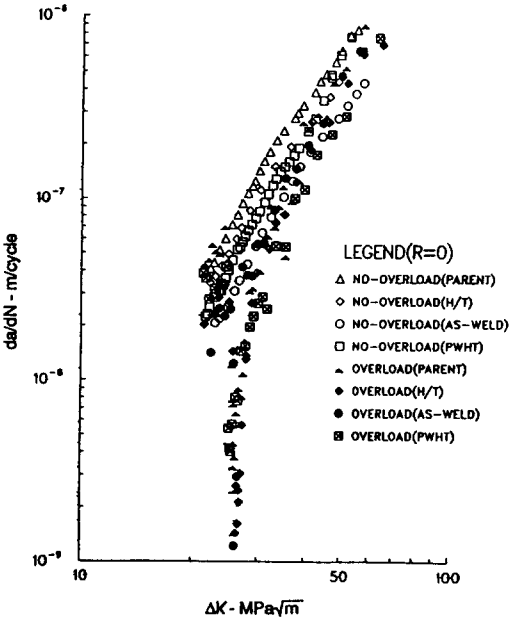

Fig. 14 Fatigue crack growth rate versus Δ K, all materials, R ≈ 0

cycle while after the single overload the rate drops to almost 10^{-9} m/cycle. Converging of the no overload and overload data occurs as the crack grows out of the effective overload region. A superposition of no overload and overload data similar to Fig. 13 is shown in Fig. 14 with R ≈ 0 and in Fig. 15 with R = 0.5 for all materials. Open data points represent no overload behavior. Greater scatter exists for the R ≈ 0 tests, however all material tests again exhibit similar behavior. Fig. 16 shows the single overload data for both R ratios. It is quite evident here, that the R ratio is the predominant factor when comparing da/dN with applied △K. Since crack closure was not monitored in these tests, an effective △K analysis cannot be made.

3.3 Fracture Surface Observation

Typical SEM fractographs for the three material conditions at both temperatures are shown in Fig. 17. Room temperature results are shown on the

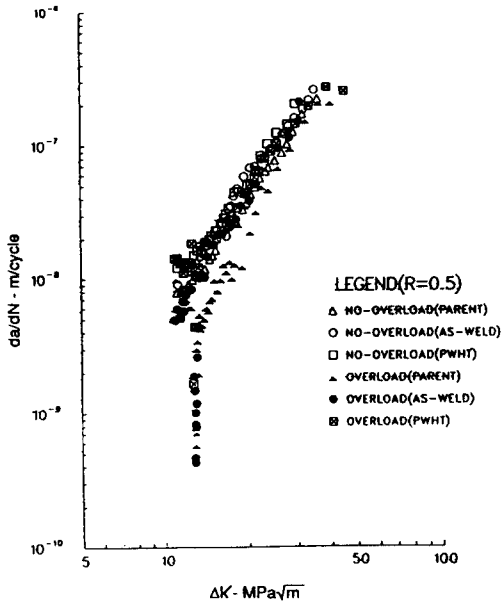

Fig. 15 Fatigue crack growth rate versus ΔK, all materials, R ≈ 0.5

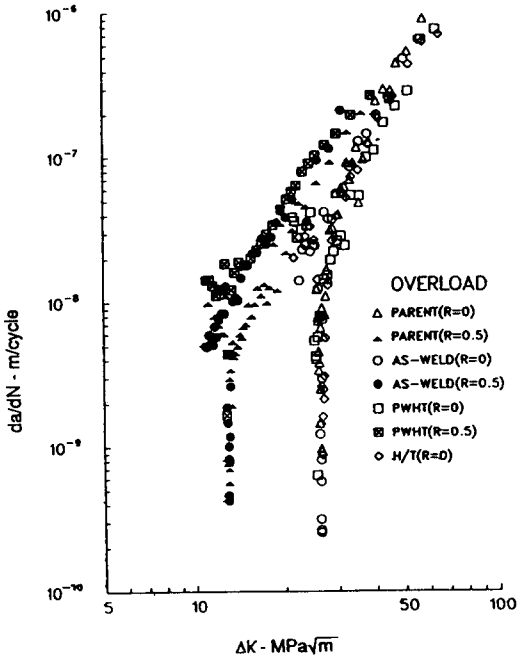

Fig. 16 Fatigue crack growth rate versus ΔK for single overloads, all materials, R ≈ 0 and 0.5

left of the figure and -45℃ results are to the right. The direction of macro fatigue crack growth is from bottom to top in all fractographs. Very few distinct striations are evident on any of the surfaces, however, at room temperature, a so-called ductile quasi-striation crack growth morphology exists. All materials show porosity, inclusions and secondary cracking and are similar at a given temperature. At -45℃, more microcracks and greater smoothness along with quasi-cleavage are evident over the fracture surfaces. These differences, however, do not cause significant temperature influence in the region constant amplitude fatigue crack growth behavior.

Fig. 18 shows the effect of the single tensile oveload for the parent, as-welded HAZ and PWHT HAZ material conditions. The left fractographs, taken at 100x or 200x magnification, show the tensile overload markings. The right fractographs show the fracture surface observed at 1000x magnification after the overload was applied. Substantial crack closure following the overload often tended to obscure some of the fatigue crack growth markings. In general, no great differences in the fatigue crack growth morphology existed between the different material conditions tested. This is consistent with the lack of substantial differences between material conditions.

4. CONCLUSIONS

The following information is based upon room temperature fatigue crack growth and SEM investigations of the 4140 parent metal, as-welded HAZ material using automatic submerged arc welding and PWHT HAZ material subjected to constant amplitude loading (no-overload) and single tensile overloads at room temperature and low temperature of -45℃ using an OLR of 2.5.

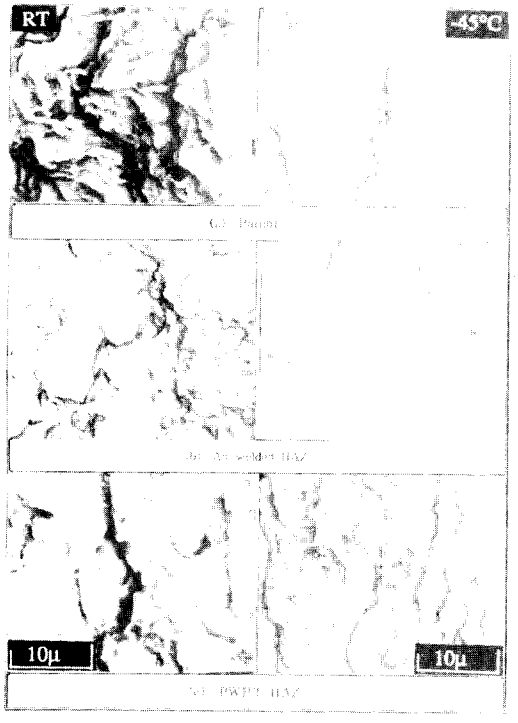

Fig. 17 Typical SEM fractographs for constant amplitude fatigue at room and low temperature
(a) parent metal (b) as-welded HAZ
(c) PWHT HAZ

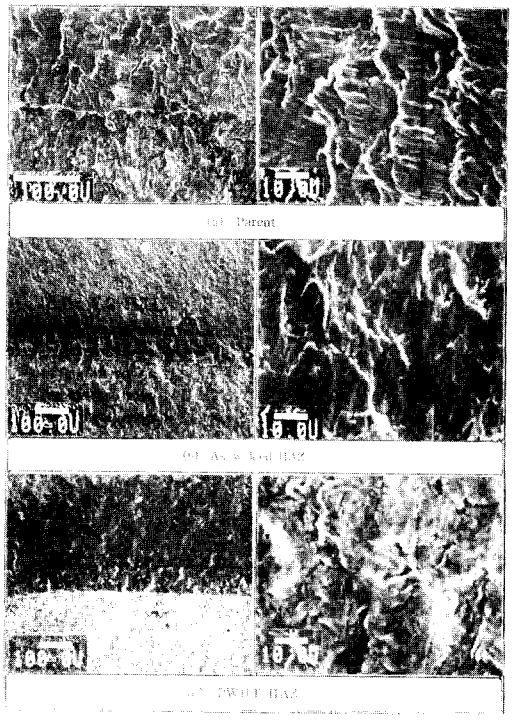

Fig. 18 Typical SEM fractographs after single overload
(a) parent (b) as-welded HAZ
(c) PWHT HAZ

1) For a given R ratio, all three material conditions, (parent Metal, as-welded HAZ, and PWHT HAZ) have essentially the same fatigue crack growth resistance at Region Ⅱ at both room temperature and -45℃. Differences in the fatigue crack growth rates for a given $\triangle K$ are less than a factor of 2.5 for $R \approx 0$ and 1.5 for $R = 0.5$.

2) The stress ratio, R, has the greatest influence on the fatigue crack growth resistance at Region Ⅱ . For a given $\triangle K$, fatigue crack growth rates with $R = 0.5$ are 1 to 4 times higher than those with $R \approx 0$.

3) Retardation of fatigue crack growth varis from 2×10^5 to 6×10^5 cycles for the four material conditions which represents an increase in fatigue crack growth life from 150 to 600 percent. The greatest retardation response occurs in the as-welded HAZ material under both $R \approx 0$ and 0.5 test conditions.

4) SEM fractography reveals similar fatigue crack growth morphology for the three material conditions at a given temperature. At -45℃, more microcracks and smoothness are evident along with quasi-cleavage.

Reference

1. Phillip, R. H., "In Situ Determination of Transformation Temperature in the Weld Heat Affected Zone", Welding Journal, Jap., 1983, pp 12s-18s.

2. Frost, R. H., Edwards, G. R. and Rheinlander, A. D., "A Constitutive Equation for the Critical Energy Input during Electroslag Welding", Welding Journal, Jap., 1982, pp 1s-6s.
3. Kameda, J., Takahashi, H. and Suzuki, M., "Residual Stress Relief and Local Embrittlement of Weld HAZ in Reaction Pressure Vessel Steel", IIW Doc. No. X-800-76 and Doc. No. IX-1002-76., 1976.
4. Dawes, M. G., "Weld Metal Fracture Toughness", Welding Journal, Dec, 1976, pp 1052-1059.
5. Lim, Jae Kyoo and Chung, Se Hi, "Stress Effect on PWHT Embrittlement", Fatigue and Fracture Testing of Weldments, ASTM STP 1058, 1990, pp 229-255.
6. Suzuki, M., Takahashi, H. and Kameda, J., "Post Weld Heat Treatment and Embrittlement of Weld HAZ in a Low Alloy Steel", Welding Journal of JWS, vol. 45, No. 1, 1976, pp6-13.
7. ASTM STP 596, Fatigue Crack Growth Under Spectrum Loads, 1976.
8. Stephens, R. I., Chung, J. H., and Glinka, G., "Low Temperature Fatigue Behavior of Steels-A Review", 1979, SAE paper No. 790517.
9. Stephens, R. I., Ed., "Fatigue at Low Temperatures", ASTM STP 857, 1985.